Resonant holographic interferometry of laser-ablation plumes

R. A. Lindley, R. M. Gilgenbach, and C. H. Ching
Intense Energy Beam Interaction Laboratory, Nuclear Engineering Department, The University of Michigan, Ann Arbor, Michigan 48109-2104

(Received 29 March 1993; accepted for publication 27 May 1993)

Two-dimensional species-resolved, holographic interferometry has been used to measure absolute-line-density profiles of KrF laser ablation plumes in vacuum and gas. Laser ablation plumes are generated by focusing a KrF excimer laser (40 ns, 248 nm, $\leqslant$0.8 J) on a solid aluminum target at a fluence of 2–5 J/cm^2. Aluminum neutral absolute-line-density profiles are measured to characterize the interaction of ablated material with background gases versus vacuum. The interferograms are made using a 20 ns pulsed dye laser tuned near ($\leqslant \pm 0.020$ nm) the 394.401 nm aluminum neutral transition from the ground state. Calculations have been performed to obtain absolute-line-density profiles from the resonant fringe shift data. Peak aluminum neutral line densities of up to 1×10^{15} cm^{-2} have been measured for plumes in backgrounds of 14 mTorr and 1 Torr argon and in vacuum.

Laser ablation has important applications in the deposition of thin films of nitride[1] and oxide materials as well as the micromachining and etching of polymers.[2] One of the crucial problems of laser ablation processing is the characterization of specific species in the ablation plume, in particular the measurement of particle density and expansion velocity. Resonant absorption spectroscopy[3,4] and hook spectroscopy[5] have been used to measure species-specific, absolute-particle-line-density along a laser beam path while planar laser-induced fluorescence[6] (PLIF) has given two-dimensional, species-specific, relative-particle-density profiles. Species-resolved expansion velocities have been measured using time of flight (TOF) emission spectroscopy,[7] direct particle collection,[8] resonant absorption,[3,4,9] laser-induced fluorescence[4,10,11] (LIF) and PLIF.[6] Plasma electron density has been measured using laser interferometry in Refs. 12 (for laser ablation) and 13 (for a laser-triggered switch), and nonresonant, ultrafast-laser photography has been used to image polymer ablation plumes.[14,15] Previous research by the authors[16,17] has utilized dye laser resonance absorption photography (DLRAP) to measure species-specific expansion velocities but did not yield particle density estimates.

In this letter, we present the first two-dimensional, species-specific, absolute-line-density profiles of excimer laser-ablated atomic aluminum neutrals using resonant holographic interferometry. These measurements have been performed in both vacuum and argon gas backgrounds at pressures of 14 mTorr and 1 Torr.

A simplified experimental configuration is shown in Fig. 1. A KrF excimer laser beam (40 ns, $\leqslant$0.8 J, 248 nm) is focused ($\approx$0.1 cm^2, 2–5 J/cm^2) onto an aluminum target inside a turbomolecular-pumped vacuum chamber to form a plume of ablated aluminum. The target is 98.5% pure aluminum and is initially ablated 20–50 times to remove oxide layers. The KrF excimer laser pulse energy is monitored by splitting off a fraction of the beam with a quartz flat (not shown) onto a calorimeter. A XeCl excimer-laser pumped dye laser (20 ns, $\approx$5 mJ), tuned near (394.401 nm$\pm\leqslant$0.020 nm) the Al(I) $3\,^2P_{1/2}$–$4\,^2S_{1/2}$ transition from ground state, is split by an uncoated, quartz interferometry flat (shown) turned 70° from normal incidence. Both beams are then focused through an iris and expanded, with the object beam passing above the aluminum surface. Additional mirrors are used to make the difference in path lengths less than the coherence length of the dye laser (estimated at about 5 cm) and recombine the two beams at a holographic plate (Agfa-Gevaert 8E56) with an angular difference of about 8°.

To make the holographic interferogram, the dye laser is pulsed twice. The ablation plume is present for one of the two dye laser pulses and a rotatable mirror in the reference beam is turned slightly between pulses to produce straight, background fringes. Four separate, double-pulsed interferograms are taken on each 4×5 in. holographic plate. A HeNe laser beam is used to reconstruct and enlarge each interferogram onto Polaroid 667 film.

The index of refraction of a neutral gas is a weak function[18] of λ except near resonances of the component atoms and molecules. For a Maxwell–Boltzmann distribution of gaseous particles in equilibrium, Measures[19] derived the fringe shift, $(\Delta s/s)$, per unit line-integrated-density, $\overline{N_i L}$, of a single resonant atomic species to be

$$\frac{(\Delta s/s)}{\overline{N_i L}} = \frac{f_{ik} r_0 c}{2\sqrt{\pi\beta}} \int_{-\infty}^{\infty} dy \, \frac{(y-u)\exp(-y^2)}{(y-u)^2+\alpha^2}, \qquad (1)$$

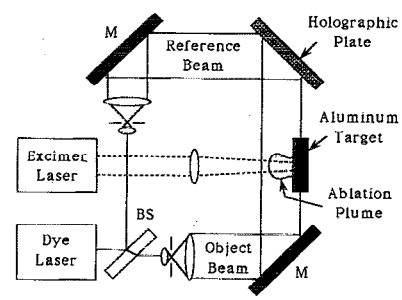

FIG. 1. Schematic of experimental configuration. Vacuum chamber not shown.

 0003-6951/93/63(7)/888/3/$6.00

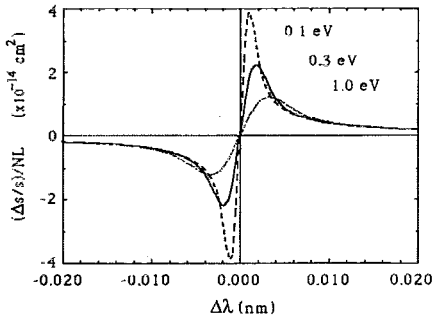

FIG. 2. Fringe shift per line density, $(\Delta s/s)/NL$, as a function of $\Delta\lambda = (\lambda - \lambda_0)$ for the neutral aluminum line $\lambda_0 = 394.401$ nm. Assumes infinitesimal laser bandwidth.

where f_{ik} is the oscillator strength of absorption for the electronic transition with wavelength λ_o, r_o is the classical electron radius,

$$\alpha = \frac{\gamma_{ik}}{2\beta}, \quad \beta = \left(\frac{2\pi}{\lambda_0}\right)\sqrt{\frac{2k_BT}{M}}, \quad y = \frac{2\pi v}{\beta\lambda_0},$$

$$u = \frac{2\pi c}{\beta\lambda_0}\left(\frac{\lambda_0 - \lambda}{\lambda_0}\right),$$

v is the particle velocity, T is the Maxwell–Boltzmann equilibrium temperature, M is the mass of the species of interest, and γ_{ik} is the damping constant, which is the sum of the natural, Lorentz, Holtzmark, and Stark broadenings. The variable, y, represents the velocity component of the resonant atoms in the direction of the propagating light and thus the integration in Eq. 1 takes into account Doppler broadening.

In this work, the plumes are considered quasi-Maxwellian in nature, with an estimated neutral temperature[10,11] in the range of 0.1–1.0 eV, and thus the above theory is applicable. In addition, a resonant ($|\Delta\lambda| \leqslant 0.020$ nm) and a nonresonant ($0.5 < |\Delta\lambda| \leqslant 1.5$ nm) holographic interferogram are taken for each experimental condition. The difference in fringe shift at each position on the holographic interferograms is then due to the resonant fringe shift given in Eq. 1. For the experimental conditions reported here, no nonresonant fringe shift was observed.

Measure's expression for $(\Delta s/s)/N_iL$ is graphed versus $\Delta\lambda$ in Fig. 2 for three different temperatures using the $3\,^2P_{1/2}$–$4\,^2S_{1/2}$ Al(I) transition from ground state, where $\lambda_0 = 394.401$ nm and $f_{ik} = 0.115$. For the experimental conditions presented here, the natural broadening is greater than the Lorentz, Holtzmark and Stark broadenings and it is small enough that the integral in Eq. 1 is insensitive to α. As shown in Fig. 2, this diagnostic is most sensitive for $|\Delta\lambda| \approx 0.002$ nm, but that is also the region of largest uncertainty due to the uncertainty in the plume temperature and the uncertainty in experimentally determining λ_0. The importance of these uncertainties diminishes for $|\Delta\lambda| > 0.005$ nm because the calculated values of $(\Delta s/s)/N_iL$ for these three plume temperatures merge together as $|\Delta\lambda|$ increases.

As Fig. 2 indicates, the direction of the fringe shift on the interferogram changes (e.g., toward or away from the target) depending on the sign of $\Delta\lambda$; this has been observed. Since the direction of the fringe shift on the interferogram is also dependent on the direction the rotatable mirror is turned, the outcome of the fringe shift on the interferograms can be predetermined. Experimentally, λ_0 is determined by taking several interferograms at wavelengths near the resonance. The interferogram with the least amount of fringe shift, the most absorption and which shows the reversal of the fringe shift direction represents λ_0 for that experimental run.

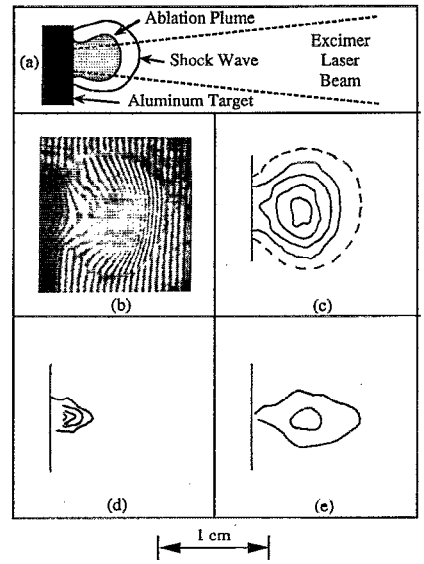

FIG. 3. (a) Photographic orientation. (b) Holographic interferogram at 4.00 μs and 1 Torr argon using $\Delta\lambda = -0.006$ nm. (c) Equiline-density profiles of (b). Dashed line is shock wave. Solid lines are single fringe shifts where each represents an incremental line-density of 1.4×10^{14} cm^{-2}. (d) Equiline-density profiles in vacuum at 0.50 μs using $\Delta\lambda = +0.010$ nm. Solid lines represent an incremental line-density of 2.4×10^{14} cm^{-2}. (e) Equline-density profiles at 1.00 μs and 14 mTorr argon using $\Delta\lambda = -0.006$ nm. Solid lines represent an incremental line-density of 1.4×10^{14} cm^{-2}. Fluence of 2–3 J/cm^2 for (b), (c), (d), and (e).

Equation (1) and Fig. 2 also assume an infinitesimal laser bandwidth. The bandwidth of our dye laser [full width at half-maximum (FWHM) of the laser intensity] is about 0.0031 nm, which is on the order of the features in Fig. 2. For large $|\Delta\lambda|$, $(\Delta s/s)/N_iL$ is nearly constant over the range of the laser bandwidth so Eq. (1) and Fig. 2 can be used directly. However, for small $|\Delta\lambda|$, $(\Delta s/s)/N_iL$ varies significantly over the range of the laser bandwidth so Eq. (1) is only useful as a rough approximation. A more detailed theory for holographic interferogram interpretation accounting for finite laser bandwidth at smaller $|\Delta\lambda|$ is presently being investigated. In this letter, it is assumed that Measure's theory is a good approximation for the wavelength range $|\Delta\lambda| \geqslant 0.006$ nm.

Figure 3(b) shows a holographic interferogram of a laser ablation plume, taken at 4.00 μs in 1 Torr of argon using $\Delta\lambda = -0.006$ nm, and Fig. 3(a) shows the photographic orientation. A shock wave is visible as a border around the ablation plume and the ablated Al neutrals are observed inside the shock front. This is consistent with Ref. 16 where ablated aluminum neutrals were observed

using DLRAP to reside within the shock wave. Unlike Ref. 16, however, shock waves were observed at 1 Torr using resonant holographic interferometry whereas shock waves were not observed below 5 Torr in Ref. 16 using DLRAP.

In order to interpret the data, fringes shift, $\Delta s/s$, is measured as the perpendicular distance a fringe has deviated from the straight, background fringes, Δs, divided by the background fringe spacing, s. Figure 3(c) shows an equiline-density profile for the interferogram shown in Fig. 3(b). The aluminum neutral plume is shaped like a mushroom cloud with a peak absolute-line-density of about 6×10^{14} cm^{-2} (assuming a plume temperature of 0.3 eV) located away from the target surface. Reference 6 attributes the mushroom shape of their copper ablation plume to the combination of exothermic condensation of the atoms to the dimer and the vortex induced by the directionally expanding laser ablation plume into the background gas. Since the diameter of the plume in Fig. 3(c)is about 1 cm, the peak average-particle-density is about 6×10^{14} cm^{-3}, which is in good agreement with recent particle density measurements using absorption spectroscopy,[3,4] hook spectroscopy,[5] and planar-laser-induced-fluorescence (PLIF).[6]

Figure 3(d) shows an equiline-density profile for an interferogram taken at 0.50 μs in vacuum (0.2 mTorr air) using $\Delta\lambda=+0.010$ nm. The blank space between the target surface and the equiline-density profile represents a section of the interferogram where the fringe shifts were unreadable due to absorption. The peak line-density in this inteferogram is about 1×10^{15} cm^{-2}, which is the maximum line-density measured in this work.

Figure 3(e) shows an equiline-density profile for an interferogram taken at 1.00 μs in 14 mTorr of argon using $\Delta\lambda=-0.006$ nm. The peak line density is about 3×10^{14} cm^{-2} and is located away from the target surface.

A time sequence of interferograms taken at all three pressures reveals that the peak line-density on a given interferogram is attached to the target surface at earlier times, detaches from the surface at a time dependent upon the background pressure and the fluence, and then moves away from the surface. As the aluminum neutrals expand and at higher background pressures form molecules, the peak aluminum neutral line-density observed decreases and the line-density profile appears to recede back to the target surface. The resonant interferogram time scans are consistent with the DLRAP pressure scans in Ref. 16, showing that plume expansion is retarded with increasing background gas pressure.

The general shape of the aluminum neutral line-density profiles is consistent within each data run, but the observed changes from run-to-run are apparently dependent upon experimental parameters such as fluence magnitude, fluence uniformity, background pressure, and the distance from the laser focal lens to the target.[6] For example, the evolution of a mushroom cloud was observed at 1 Torr while the evolution of an asymmetric, expanding ellipsoid was observed in vacuum.

In conclusion, the resonant holographic interferometry diagnostic has been shown to yield absolute-line-density profiles of laser-ablated neutral aluminum plumes in vacuum and in argon at pressures of 14 mTorr and 1 Torr. This diagnostic should prove useful to applications including laser-machining and laser-ablative deposition of thin films. Resonant holographic interferometry has been used by the authors at higher pressures of argon (35 Torr) and in argon rf plasmas. These results will be presented in a future paper.

This research is supported by National Science Foundation Grant CTS-9108971. R. A. L has a Magnetic Fusion Energy Technology fellowship which is administered for the U. S. Department of Energy by Oak Ridge Associated Universities. The authors acknowledge the technical assistance of D. Love, J. Lash, A. Allen, and R. Schmitz and the helpful discussions with R. C. Hazelton, Y. Y. Lau, D. Steel, and J. Geddes.

[1] G. L. Doll and J. A. Sell, Phys. Rev. B **43**, 6816 (1991).
[2] R. Srinivasan and B. Braren, J. Polymer Sci.: Polymer Chem. Ed. **22**, 2601 (1984).
[3] N. H. Cheung, Q. Y. Ying, J. P. Zheng, and H. S. Kowk, J. Appl. Phys. **69**, 6349 (1991).
[4] A. D. Sappey and T. K. Gamble, Appl. Phys. B **53**, 353 (1991).
[5] A. D. Sappey, T. K. Gamble, and D. K. Zerkle, Appl. Phys. Lett. **62**, 564 (1993).
[6] A. D. Sappey and T. K. Gamble, J. Appl. Phys. **72**, 5095 (1992).
[7] K. Murakami, in *Laser Ablation of Electronic Materials*, edited by E. Fogarassy and S. Lazare (Elsevier, Amsterdam, 1992).
[8] S. C. Langford, J. T. Dickinson, and L. C. Jenson, J. Appl. Phys. **62**, 1437 (1987).
[9] D. B. Geohegan and D. N. Mashburn, Appl. Phys. Lett. **55**, 2345 (1989).
[10] R. W. Dreyfus, R. Kelly, and R. E. Walkup, Appl. Phys. Lett. **49**, 1478 (1986).
[11] R. W. Dreyfus, J. Appl. Phys. **69**, 1721 (1991).
[12] R. E. Walkup, J. M. Jasinski, and R. W. Dreyfus, Appl. Phys. Lett. **48**, 1690 (1986).
[13] W. D. Kimura, M. J. Kushner, E. A. Crawford, and S. R. Bryon, IEEE Trans. Plasma Sci. **PS-14**, 246 (1986).
[14] A. Gupta, B. Braren, K. G. Casey, B. W. Hussey, and R. Kelly, Appl. Phys. Lett. **59**, 1302 (1991).
[15] T. Zyung, H. Kim, J. C. Postlewaite, and D. D. Dlott, J. Appl. Phys. **65**, 4548 (1989).
[16] P. L. G. Ventzek, R. M. Gilgenbach, C. H. Ching, and R. A. Lindley, J. Appl. Phys. **72**, 1696 (1992).
[17] R. M. Gilgenbach and P. L. G. Ventzek, Appl. Phys. Lett. **58**, 1597 (1991).
[18] C. M. Vest, *Holographic Interferometry* (Wiley, New York, 1979).
[19] R. M. Measures, Appl. Opt. **9**, 737 (1970).